GEOPHYSICAL RESEARCH LETTERS, VOL. 32, L17102, doi:10.1029/2005GL023353, 2005

Storm-time plasma signatures observed by IMAGE/MENA and comparison with a global physics-based model

M. H. Denton,[1] V. K. Jordanova,[2] M. G. Henderson,[1] R. M. Skoug,[1] M. F. Thomsen,[1] C. J. Pollock,[3] S. Zaharia,[1] and H. O. Funsten[1]

Received 27 April 2005; revised 13 June 2005; accepted 2 August 2005; published 3 September 2005.

[1] We present energetic neutral atom (ENA) fluxes measured by the medium energy neutral atom (MENA) imager onboard the IMAGE satellite for the geomagnetic storm of 21 October 2001 at energies of 6 and 12 keV. The fluxes indicate strong low altitude emissions close to the Earth and a nightside peak close to local midnight. The fluxes are compared with theoretical ENA fluxes calculated using the ring current-atmosphere interaction model (RAM). We find good quantitative agreement between MENA data and RAM results, both of which indicate a peak in ENA emissions on the nightside, close to local midnight which varies in radial location between ~2 and ~5 R_e during the period of study. We demonstrate the validity of comparing RAM results with MENA data and pave the way for further study of plasma sheet entry to the inner magnetosphere during storm-times. **Citation:** Denton, M. H., V. K. Jordanova, M. G. Henderson, R. M. Skoug, M. F. Thomsen, C. J. Pollock, S. Zaharia, and H. O. Funsten (2005), Storm-time plasma signatures observed by IMAGE/MENA and comparison with a global physics-based model, *Geophys. Res. Lett.*, *32*, L17102, doi:10.1029/2005GL023353.

1. Introduction

[2] Energetic neutral atom (ENA) imaging in the magnetosphere relies on charge-exchange reactions between energetic ions and cold atoms constituting the neutral geocorona and upper atmosphere. Each reaction allows a neutral atom to exit the collision with high velocity as an ENA propagating unconstrained by magnetic and electric fields. Therefore ENAs can be used to image the ring current and plasma sheet remotely by instruments such as the medium energy neutral atom (MENA) imager on-board the IMAGE satellite. The goal of this instrument is to derive the distribution function of magnetospheric ions. Since the medium is optically thin, MENA data are a measurement of the line-of-sight ENA flux at a given energy. Inversion of images can then be used to give the ion flux, assuming an accurate model of the geocoronal neutral density [*Perez et al.*, 2001; *DeMagistre et al.*, 2004]. Thus ENA imaging provides a tool with which to view a snapshot of the global ion population of the magnetosphere and is a complementary technique to in situ measurements.

[3] ENA imaging as a tool for investigating magnetospheric structure was first proposed by *Hovestadt and Scholer* [1976] and demonstrated experimentally by *Roelof* [1987]. A review by *Williams et al.* [1992] summarized the field of ENA imaging in relation to other magnetosphere imaging techniques. *Lui et al.* [1996, 2001] provided first composition measurement of ENAs and numerous studies have demonstrated the usefulness of ENA imaging including observations from the first dedicated ENA imager onboard the Astrid satellite [*Brandt et al.*, 1997]. The first images of ENA emissions using POLAR/CEPPAD were reported by *Henderson et al.* [1997] who also reported ENA emissions during periods of substorm activity [*Henderson et al.*, 2000]. High energy neutral atom (HENA) imager data have successfully been used to analyze substorm injections and the storm time ring current [e.g., *Brandt et al.*, 2002].

[4] Resolving the plasma structure of the magnetosphere using ENA imagers is a primary scientific goal of the IMAGE mission [*Burch*, 2000]. MENA detects energetic neutral atoms between 1 and ~45 keV [e.g., *Pollock et al.*, 2000, *McComas et al.*, 2002]. The aim of this paper is to investigate how plasma sheet material is delivered to the inner magnetosphere during storms. A peak in ENA emissions is an indicator of a peak in the ion population and thus MENA data can be used to quantify the location of the peak ENA flux, tracing how the ion population at a given energy evolves during storms. We present storm-time ENA fluxes observed by MENA and for the first time present quantitative comparisons between MENA measured flux and the neutral flux calculated using a global, physics-based, ring-current model.

[5] Previous studies have compared ENA images with model data but there is no consensus on whether the location of peak flux occurs in the pre- or post-midnight sectors. *Brandt et al.* [2002] used HENA observations in the 27–39 keV range to show the ENA peak, in response to large excursions in IMF-B_y, may rotate to the dawn region during the mainphase. Recent work by *Le et al.* [2004] shows that for large Dst storms the peak in ion flux, and by implication the ENA flux, occurs near dusk whilst *Lui* [2003] showed the peak plasma pressure is located in the pre-midnight sector, implying a pre-midnight peak in the ion distribution although neither study separated main phase from recovery phase. It remains unclear how the peak in ENA flux evolves temporally throughout a storm, although *Ebihara et al.* [2002] showed statistical results from POLAR indicating that the main and recovery phases are likely to be different in the energy range 1–200 keV.

[1]Space and Atmospheric Sciences, Los Alamos National Laboratory, Los Alamos, New Mexico, USA.
[2]Space Science Center, University of New Hampshire, Durham, New Hampshire, USA.
[3]Instrumentation and Space Research Division, Southwest Research Institute, San Antonio, Texas, USA.

0094-8276/05/2005GL023353$05.00

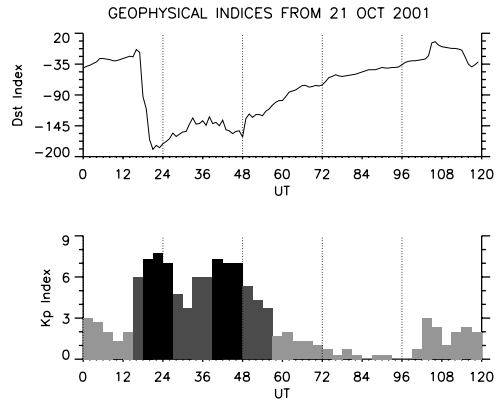

Figure 1. Dst and Kp indices plotted for five days in October 2001. The storm is characterized by a sudden onset, a sharp fall to minimum Dst, an extended period of sawtooth activity and a smooth recovery phase.

[6] For comparison with MENA data, the ring current-atmosphere interaction (RAM) model [e.g., *Jordanova et al.*, 1997] is used to produce equatorial ion distributions at the time of MENA observations. Model data are then mapped along dipolar magnetic field lines using Liouville's Theorem. Since RAM calculates the pitch angles of the ring current ions, it is possible to map the local pitch angle at the point where the line-of-sight intersects a given field line, to the corresponding pitch angle at the equator, to provide the global ion distribution. We interpolate RAM flux at a given energy to calculate ion flux at the line-of-sight intersection. ENA images are produced from this distribution by calculating the line-of-sight integral ENA flux.

[7] The Geospace Environment Modeling Inner Magnetosphere-Storm (GEM IM-S) challenge describes criteria for comparison of ENA observations with ring current models. The 21 October 2001 storm is one of two storms selected for the challenge which states that comparison between observations and models should be carried out in the first instance by comparing the location of the peak ENA flux at a given energy. The work presented in this paper is in part carried out in response to the challenge.

2. Analysis

[8] MENA data are analyzed using a recently developed technique which allows calculation of the differential energy ENA flux [*Henderson et al.*, 2005]. The method is a significant improvement in MENA data processing and was developed by re-deriving the instrument's geometric factor and applying appropriate calibration information.

[9] The RAM model has been described by *Jordanova et al.* [1997]. In brief, for a dipolar field, the bounce-averaged kinetic equation is solved to provide the ionized H^+ flux in the equatorial plane, taking account of charge-exchange losses with neutral hydrogen and Coulomb collisions with the thermal population. Wave-particle interactions are neglected in this study. The magnetospheric electric field is provided by taking the gradient of a Kp-dependent Volland-Stern (RAM-VS) or Weimer (RAM-W) potential model. LANL geosynchronous satellite data are used as boundary conditions to the model. RAM has previously been used to study other storms [*Jordanova et al.*, 2001, 2003] and recent work by *Zaharia et al.* [2005] shows how RAM pressures can be used as input to a 3-D equilibrium code.

[10] The validity of modeling an assumed ring current distribution to produce ENA images has been demonstrated by *Henderson et al.* [1999]. Here, a modified version of their software tool (developed for use with Polar/CEPPAD) is used to investigate ENA fluxes that would be observed by MENA given an equatorial ion distribution provided by RAM. Such modeling is valuable as a step toward the ultimate goal of inverting MENA images to provide the global ion distribution directly.

[11] ENA fluxes based on RAM equatorial ion fluxes are calculated for a given energy at L = 2 to L = 6.5 for all MLT and all pitch angles. To provide an ion distribution in regions beyond the bounds of the model (L < 2.0 and L > 6.5) we assume the equatorial ion density inward of L = 2.0 falls off linearly with distance from its value at the boundary. Outward of L = 6.5, the density is set to its value at L = 6.5. We assume the sole constituent of the geocorona is H^+ with a neutral atmosphere provided by the *Chamberlain* [1963] model with parameters determined by *Rairden et al.* [1986].

3. Results

[12] Storm onset occurred at ~16 UT on 21 October 2001 (see Figure 1) and a high energy penetrating particle background contaminates MENA data at the start of the storm. Contamination is present during the first day of the storm at a level that falls with time after storm onset. As a result of this, and the characteristics of MENA the highest count rates are obtained near the lower end of the 1–40 keV energy range. Since our interest is how plasma sheet material is injected during storms, and then goes on to form the ring current, energies of 6 and 12 keV are used in this study.

[13] For the period preceding the storm, IMF-B_z was slightly negative (~−5 nT) with IMF-B_y positive and fairly steady (~+5 nT). To illustrate the data/model comparison, data from 18–24 UT are analyzed. This period is considered representative of main phase storm activity and useful for initial comparison of observations and theory. Figure 2 shows example MENA and RAM-VS fluxes at 6 keV. The MENA fluxes are a 60 minute integration from 20–21 UT. A shorter integration time would be preferable but is not possible for this storm due to the high background noted above. The RAM-VS fluxes are calculated using the forward modeling tool of *Henderson et al.* [1999]. The images in Figure 2 are overlaid on the solar-magnetic (SM) x-y plane. The red axis is the positive x-axis and each grid square is 2 × 2 R_e in size.

[14] The MENA and model images show strong peaks in ENA emissions close to the Earth, and extended emissions on the nightside. At low altitudes the ENA flux increases dramatically due to the increased neutral density of the upper atmosphere. Bright pixels close to Earth are associated with such "low altitude emissions"

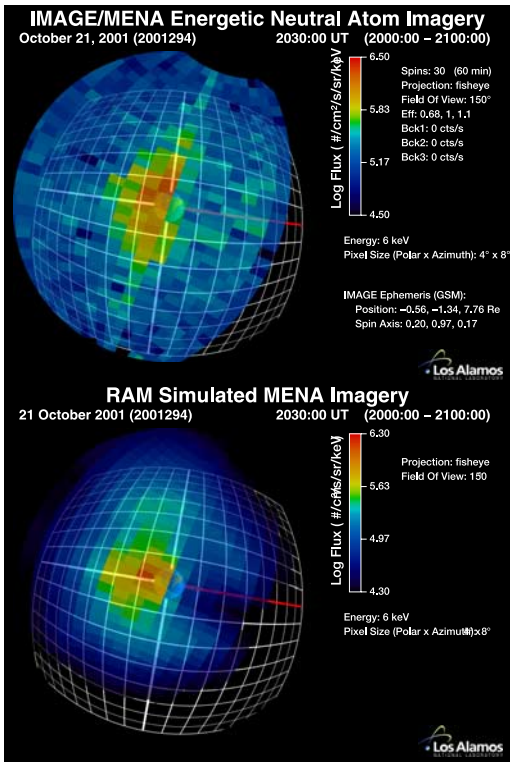

Figure 2. The measured MENA and modeled RAM-VS fluxes at 6 keV between 20–21 UT on 21 October 2001.

[*Roelof*, 1997; *Pollock et al.*, 2001; *Brandt et al.*, 2001]. However, in MENA saturation of one pixel may occur and spread to adjacent pixels in the polar direction [*Pollock et al.*, 2001]. Such "blooming" exaggerates flux in pixels adjacent to those closest to Earth along the dawn-dusk line. To avoid bias we neglect regions where blooming and low altitude emissions occur. We determine the peak flux location between $y = \pm 6.5$ and $x < -2$ in the SM x-y plane. Examination of MENA images leads us to conclude that we remove regions of blooming without removing valid data thus locating the peak ENA flux primarily associated with storm processes. Due to the severe nature of the storm, the effects of a high background remain and MENA flux is elevated, although in a way that may not be uniform across the image [*Henderson et al.*, 2005]. Solely for this study, we assume a uniform background which does not affect the measured peak ENA flux location.

[15] To provide a quantitative measure of the agreement between experiment and theory we adopt the criterion selected at the GEM 2004 Workshop; namely that agreement between model results and ENA observations should, in the first instance, be sought by matching the modeled equatorial plane location of the peak in ENA emissions with the observed location. The location of the peak emissions is calculated by determining the intersection of the MENA all-sky image with the equatorial plane and then calculating the point with the highest flux in this plane. Figure 3 shows the location of peak emissions measured by MENA and calculated by RAM-VS and RAM-W at 6 and 12 keV, from 18–24 UT. The measured peak at 6 keV is located in the post-midnight sector, close to local midnight, whilst the peak at 12 keV is located further duskwards, in the pre-midnight sector. RAM-VS gives an ENA peak closer to the measured value, whilst RAM-W shows an ENA peak further duskwards than that measured by MENA.

4. Discussion and Conclusions

[16] The experimental and model results in Figure 2 show similar spatial features, namely high ENA flux close to the Earth, with flux decreasing radially from the Earth and maximized on the nightside, close to local midnight. The peak in ENA emissions measured by MENA varies radially, and to a lesser extent, with local time, throughout the storm although the magnitude of the flux at a given energy is roughly constant between 18–24 UT. We interpret this as indicative of plasma sheet material entering the inner magnetosphere during the time of the observations. The peak at 12 keV is located duskwards of the peak at 6 keV and this may be expected since lower energy ions respond more to the electric field than the magnetic field. Peaks in the magnitude of ENA flux do occur at other times during the storm, possibly due to injections associated with sawtooth activity.

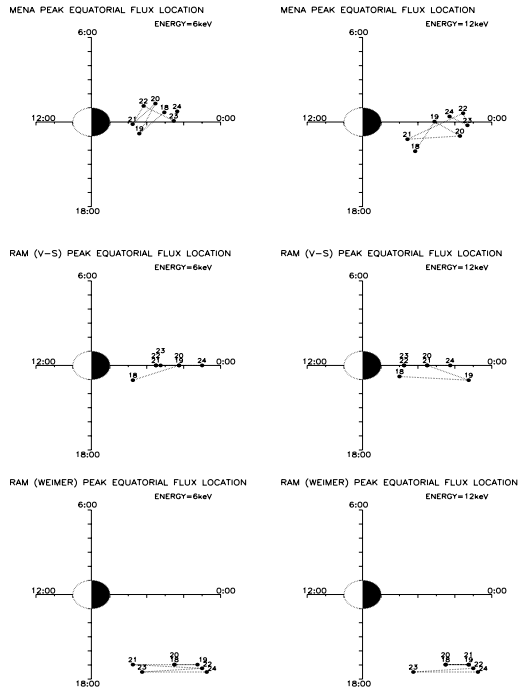

Figure 3. Plots of the location of peak ENA flux in the SM-xy plane at 6 and 12 keV as measured by MENA and calculated by RAM-VS and RAM-W on 21 October 2001 at 18–24 UT (UT is given by the numbering of the points). Excluding bright spots associated with low altitude emissions, the peak ENA flux measured by MENA and calculated by RAM-VS is found on the nightside close to local midnight. (Note: the location of peak RAM-VS ENA fluxes in many cases is directly on the x-axis).

[17] The ENA peak flux is located close to local midnight during the period of study and although it moves radially during the storm, neither MENA nor RAM-VS indicate a large variation in the local time location of the peak ENA flux at a specific energy. This implies the peak density of the injected plasma sheet material also varies mostly in the radial direction during the storm. RAM-VS results show the ENA peak located close to local midnight in a similar location to that detected by MENA. Additional calculations for the storm study presented by *Zaharia et al.* [2005] indicate that the pressures calculated by RAM-W are unrealistic although the model does reproduce the actual Dst variation of the storm quite well. Neither RAM-VS or RAM-W shows a large energy dependence of the peak ENA location at 6 or 12 keV although both models predict further duskwards movement of the ENA peak at higher energies.

[18] *Le et al.* [2004] showed the peak equatorial ring current intensity is located close to local midnight for small storms ($-20 > Dst^* > -40$ nT), moving duskwards for larger storms, although the authors did not examine if differences exist between main phase and recovery. *Brandt et al.* [2002] used HENA to propose a possible IMF-B_y dependence to the local time location of the ENA peak in the energy range 27–39 keV. They found instances where the peak flux rotated toward dawn for strongly positive IMF-B_y. Further study is required to determine if this effect occurs at energies in the MENA range although preliminary study of other storms indicates the peak ENA emissions in the MENA range can indeed be found in the post-midnight sector. The body of work on this subject, including the current study, indicates that the location of peak flux is energy dependent, but variables such as IMF orientation and storm strength are not negligible. We conclude by noting the agreement found between MENA and RAM-VS gives confidence to apply our method in future studies.

5. Summary and Future Work

[19] We have used the storm of 21 October 2001 to develop a technique of comparing experimental to theoretically derived ENA fluxes. The storm is one of two chosen for the 2004 GEM IM-S challenge, one aim of which is to compare output from ring current models to ENA observations. MENA observations are not optimal for this storm and high count rates at the start of the event limit the usefulness of observations at this time. Despite this we find broad agreement between theory and experiment.

[20] For the main phase of the 21 October 2001 storm we find:

[21] 1. The peak in ENA emissions at energies of 6 and 12 keV is located close to local midnight.

[22] 2. The measured peak flux at 12 keV is located duskwards of the peak flux at 6 keV. The peak flux location varies in radial location from $\sim$2 to $\sim$5 R_e during the period of study.

[23] 3. A sophisticated ring current model predicts ENA images similar to MENA images, with the peak equatorial flux at 6 and 12 keV located close to local midnight.

[24] The RAM predictions of the global ENA distribution lead us to conclude that the ion fluxes provided by the model are reliable in these circumstances. Further comparisons to determine how, and in what way, the flux of ENAs observed by MENA during storms is spatially, temporally and energy dependent are planned. We also aim to test the use of more sophisticated field and potential models and to address the question of how ENAs respond during the prestorm and recovery phases.

[25] **Acknowledgments.** Work at LANL was performed under the auspices of the US Department of Energy with support from the NASA IMAGE program. Work at UNH was supported by NASA grant NAG5-13512. The authors thank WDC-C1 at RAL for the geomagnetic indices, and P. H. Janzen for helpful discussions.

References

Brandt, P. C., et al. (1997), ENA imaging from the Swedish microsatellite Astrid during the magnetic storm of 8 February 1995, *Adv. Space Res.*, *20*, 1061–1066.

Brandt, P. C., et al. (2001), ENA imaging at low altitudes from the Swedish microsatellite Astrid: Extraction of the equatorial ion distribution, *J. Geophys. Res.*, *106*, 25,731–25,744.

Brandt, P. C., et al. (2002), Global ENA observations of the storm mainphase ring current: Implications for skewed electric fields in the inner magnetosphere, *Geophys. Res. Lett.*, *29*(20), 1954, doi:10.1029/2002GL015160.

Burch, J. L. (2000), IMAGE Mission overview, *Space Sci. Rev.*, *91*, 1–14.

Chamberlain, J. W. (1963), Planetary coronae and atmospheric evolution, *Planet. Space Sci.*, *11*, 901–960.

DeMagistre, R., et al. (2004), Retrieval of global magnetospheric ion distributions from high energy neutral atom (ENA) measurements by the IMAGE/HENA instrument, *J. Geophys. Res.*, *109*, A04214, doi:10.1029/2003JA010322.

Ebihara, Y., et al. (2002), Statistical distribution of the storm-time proton ring current: POLAR measurements, *Geophys. Res. Lett.*, *29*(20), 1969, doi:10.1029/2002GL015430.

Henderson, M. G., et al. (1997), First energetic neutral atom images from Polar, *Geophys. Res. Lett.*, *24*, 1167–1170.

Henderson, M. G., et al. (1999), Energetic neutral atom imaging with the POLAR CEPPAD/IPS instrument: Initial forward modeling results, *Phys. Chem. Earth*, *24*, 203–208.

Henderson, M. G., et al. (2000), POLAR CEPPAD/IPS energetic neutral atom (ENA) images of a substorm injection, *Adv. Space Res.*, *25*, 2407–2416.

Henderson, M. G., et al. (2005), Calculation of IMAGE/MENA geometric factors and conversion of images to units of integral and differential flux, *Rev. Sci. Instrum.*, *76*, 43303, 1–24.

Hovestadt, D., and M. Scholer (1976), Radiation belt-produced energetic hydrogen in interplanetary space, *J. Geophys. Res.*, *81*, 5039–5042.

Jordanova, V. K., et al. (1997), Kinetic model of the ring current-atmosphere interactions, *J. Geophys. Res.*, *102*, 14,279–14,291.

Jordanova, V. K., et al. (2001), Ring current dynamics during the 13–18 July 2000 storm period, *Sol. Phys.*, *204*, 361–375.

Jordanova, V. K., et al. (2003), Effects of plasma sheet variability on the fast initial ring current decay, *Geophys. Res. Lett.*, *30*(6), 1311, doi:10.1029/2002GL016576.

Le, G., et al. (2004), Morphology of the ring current derived from magnetic field observations, *Ann. Geophys.*, *22*, 1267–1295.

Lui, A. T. Y. (2003), Inner magnetospheric plasma pressure distribution and its local time asymmetry, *Geophys. Res. Lett.*, *30*(16), 1846, doi:10.1029/2003GL017596.

Lui, A. T. Y., et al. (1996), First composition measurements of energetic neutral atoms, *Geophys. Res. Lett.*, *23*(19), 2641–2644.

Lui, A. T. Y., et al. (2001), Composition of energetic neutral atoms during a storm main phase, *Geophys. Res. Lett.*, *28*(7), 1363–1366.

McComas, D. J., et al. (2002), Filling and emptying of the plasma sheet: Remote observations with 1–70 keV energetic neutral atoms, *Geophys. Res. Lett.*, *29*(22), 2079, doi:10.1029/2002GL016153.

Perez, J. D., et al. (2001), Initial ion pitch angle distributions from energetic neutral atom images obtained by IMAGE, *Geophys. Res. Lett.*, *28*(6), 155–1158.

Pollock, C. J., et al. (2000), Medium energy neutral atom (MENA) imager for the IMAGE mission, *Space Sci. Rev.*, *91*, 112–154.

Pollock, C. J., et al. (2001), First medium energy neutral atom (MENA) images of Earth's magnetosphere during substorm and storm-time, *Geophys. Res. Lett.*, *28*(6), 1147–1150.

Rairden, R. L., et al. (1986), Geocoronal imaging with Dynamics Explorer, *J. Geophys. Res.*, *91*, 13,613–13,630.

Roelof, E. C. (1987), Energetic neutral atom image of a storm-time ring current, *Geophys. Res. Lett.*, *14*(6), 652–655.

Roelof, E. C. (1997), Emissions from nearly mirroring magnetospheric ions interacting with the exobase, *Adv. Space Res.*, *20*, 361–366.

Williams, D. J., et al. (1992), Global magnetospheric imaging, *Rev. Geophys.*, *30*, 183–186.

Zaharia, S., et al. (2005), Effect of storm-time plasma pressure on the magnetic field in the inner magnetosphere, *Geophys. Res. Lett.*, *32*, L03102, doi:10.1029/2004GL021491.

M. H. Denton, H. O. Funsten, M. G. Henderson, M. F. Thomsen, R. M. Skoug, and S. Zaharia, LANL, Space and Atmospheric Sciences, MS-D466, Los Alamos, NM 87545, USA. (mhdenton@lanl.gov)

V. K. Jordanova, Space Science Center, University of New Hampshire, Morse Hall, Room 410, Durham, NH 03824, USA.

C. J. Pollock, Instrumentation and Space Research Division, Southwest Research Institute, San Antonio, TX 78238, USA.